Int. J. Solids Structures Vol. 27, No. 14, pp. 1855–1865, 1991
Printed in Great Britain.

0020-7683/91 $3.00 + .00

KINKED CRACKS IN AN ANISOTROPIC PLANE MODELED BY AN INTEGRAL EQUATION METHOD

W. L. ZANG
Department of Solid Mechanics, Royal Institute of Technology, S-100 44 Stockholm, Sweden

and

P. GUDMUNDSON
SICOMP, Swedish Institute of Composites, Box 271, S-941 26 Piteå, Sweden

(*Received* 2 *April* 1990; *in revised form* 31 *August* 1990)

Abstract—A boundary integral method for cracks in an anisotropic material is presented. The method is based on the integral equation for the resultant forces along the cracks. The integral kernels contain only a weak logarithmic singularity, which simplifies the numerical implementation. Crack closure is also taken into account in the numerical formulation. Numerical tests are presented to illustrate the efficiency and the reliability of the proposed method.

1. INTRODUCTION

The increased use of composite materials has resulted in a growing interest in crack problems in anisotropic materials, see for example, the papers by Sih *et al.* (1965), Bowie and Freese (1972), Delale and Erdogan (1977), Cinar and Erdogan (1982) and Mishra and Misra (1983). It is known that the boundary integral method is very efficient for the solution of linear elastic crack problems. However, most of the results for cracks in an anisotropic medium are based on equations which are derived by using the integral transform method. This technique limits the application to rather simple geometries. A numerical method which is easy to apply and valid for more general crack configurations would be very useful for fracture investigations.

In recent years, three different kinds of boundary integral equations have been applied to crack problems in a two-dimensional isotropic elastic medium. The first kind of equation is an integral equation for the displacements on the boundary, the standard boundary element method (BEM) (cf. Brebbia *et al.*, 1984). The second kind of equation is an integral expression for tractions on the crack surfaces (cf. Zang and Gudmundson, 1988) and the third kind of equation is an integral equation for resultant forces along the crack surfaces (cf. Cheung and Chen, 1987; Zang and Gudmundson, 1989a,b, 1990). As a comparison with the other two kinds of equations, the resultant force type equation has some advantages. Unlike the standard BEM, geometrical sectioning is no longer required by employing the resultant force type equation. The unknowns of the problems can thus be significantly reduced. In addition, the integral kernels in the equation contain a weak logarithmic singularity, which is very easy to handle in the numerical calculation. It can also be proved that the equation is valid for every point along the crack, which will simplify the selection of the collocation points. Numerical tests by Cheung and Chen (1987) and Zang and Gudmundson (1989a, b, 1990) indicate that the method employing the resultant force type equation is probably the most efficient and reliable method for the solution of kinked crack problems.

In the present paper, a boundary integral equation for the resultant forces along crack lines with arbitrary crack configuration in a rectilinearly anisotropic plane is derived. A numerical implementation similar to the method by Zang and Gudmundson (1989a) is employed to solve the equation. Crack closure is also taken into account by using the same numerical algorithm presented by Zang and Gudmundson (1990). Numerical tests are presented to illustrate the efficiency and reliability of the proposed method.

2. THEORETICAL BASIS AND NUMERICAL IMPLEMENTATION

In the present study, plane anisotropic materials are considered. The generalized Hooke's law for problems without coupling between out-of plane shear and in-plane stresses can be written as (cf. Lekhnitskii, 1981)

$$\begin{aligned}
\varepsilon_x &= \alpha_{11}\sigma_x + \alpha_{12}\sigma_y + \alpha_{13}\sigma_z + \alpha_{16}\tau_{xy},\\
\varepsilon_y &= \alpha_{12}\sigma_x + \alpha_{22}\sigma_y + \alpha_{23}\sigma_z + \alpha_{26}\tau_{xy},\\
\varepsilon_z &= \alpha_{13}\sigma_x + \alpha_{23}\sigma_y + \alpha_{33}\sigma_z,\\
\gamma_{xy} &= \alpha_{16}\sigma_x + \alpha_{26}\sigma_y + \alpha_{66}\tau_{xy};
\end{aligned} \tag{1}$$

or for plane strain and stress

$$\begin{aligned}
\varepsilon_x &= \beta_{11}\sigma_x + \beta_{12}\sigma_y + \beta_{16}\tau_{xy},\\
\varepsilon_y &= \beta_{12}\sigma_x + \beta_{22}\sigma_y + \beta_{26}\tau_{xy},\\
\gamma_{xy} &= \beta_{16}\sigma_x + \beta_{26}\sigma_y + \beta_{66}\tau_{xy},
\end{aligned} \tag{2}$$

where for plane strain deformation problems

$$\begin{aligned}
\beta_{ij} &= \alpha_{ij} - \alpha_{i3}\alpha_{j3}/\alpha_{33} \quad (\alpha_{ij} = \alpha_{ji}),\\
\varepsilon_z &= 0,
\end{aligned} \tag{3}$$

and for plane stress problems

$$\begin{aligned}
\beta_{ij} &= \alpha_{ij},\\
\sigma_z &= 0.
\end{aligned} \tag{4}$$

For an orthotropic material with the material principal directions coinciding with the coordinate axes, eqn (1) reads

$$\begin{aligned}
\varepsilon_x &= \sigma_x/E_1 - \nu_{12}\sigma_y/E_2 - \nu_{13}\sigma_z/E_3,\\
\varepsilon_y &= -\nu_{21}\sigma_x/E_1 + \sigma_y/E_2 - \nu_{23}\sigma_z/E_3,\\
\varepsilon_z &= -\nu_{31}\sigma_x/E_1 - \nu_{32}\sigma_y/E_2 + \sigma_z/E_3,\\
\gamma_{xy} &= \tau_{xy}/G_{12}.
\end{aligned} \tag{5}$$

In eqn (5), Poisson's ratios and Young's moduli satisfy the following relation

$$\nu_{kj}/E_j = \nu_{jk}/E_k \quad \text{(no sum of } k \text{ and } j\text{)}. \tag{6}$$

The problem can be formulated by employing complex potentials (Lekhnitskii, 1981). The components of the displacements, the stresses and the resultant forces can be expressed as

$$\begin{aligned}
u_x &= 2\,\mathrm{Re}\,[p_1\Phi_1(z_1) + p_2\Phi_2(z_2)],\\
u_y &= 2\,\mathrm{Re}\,[q_1\Phi_1(z_1) + q_2\Phi_2(z_2)],\\
\sigma_x &= 2\,\mathrm{Re}\,[\mu_1^2\Phi_1'(z_1) + \mu_2^2\Phi_2'(z_2)],\\
\sigma_y &= 2\,\mathrm{Re}\,[\Phi_1'(z_1) + \Phi_2'(z_2)],\\
\tau_{xy} &= -2\,\mathrm{Re}\,[\mu_1\Phi_1'(z_1) + \mu_2\Phi_2'(z_2)],\\
F_x &= +2\,\mathrm{Re}\,[\mu_1\Phi_1(z_1) + \mu_2\Phi_2(z_2)] + C_1,\\
F_y &= -2\,\mathrm{Re}\,[\Phi_1(z_1) + \Phi_2(z_2)] + C_2,
\end{aligned} \tag{7}$$

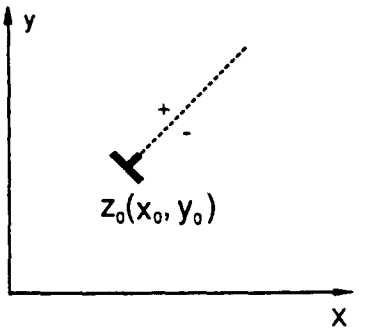

Fig. 1. An edge dislocation in an anisotropic plane.

where

$$p_j = \beta_{11}\mu_j^2 + \beta_{12} - \beta_{16}\mu_j,$$
$$q_j = \beta_{12}\mu_j + \beta_{22}/\mu_j - \beta_{26},$$
$$z_j = x + \mu_j y \quad (j = 1, 2). \tag{8}$$

In eqn (7), the primes denote the derivatives with respect to the arguments, C_j is an arbitrary real constant and μ_j is a root of the following characteristic equation

$$\beta_{11}\mu^4 - 2\beta_{16}\mu^3 + (2\beta_{12} + \beta_{66})\mu^2 - 2\beta_{26}\mu + \beta_{22} = 0. \tag{9}$$

It has been shown by Lekhnitskii (1981) that the roots of eqn (9) can never be real. For a particular material, the roots of eqn (9) can thus be chosen as

$$\bar{\mu}_3 = \mu_1, \quad \bar{\mu}_4 = \mu_2, \tag{10}$$

where bars denote complex conjugation.

It is now assumed that an edge dislocation is located at a point $z_0(x_0, y_0)$, see Fig. 1. If the plane is cut by a straight line from the point z_0 to infinity, an upper side and a lower side of the line can be defined, see also Fig. 1. The phase angle will thus change by 2π if the point z_0 is encircled from the lower to the upper side of the line. For a particular material, the roots μ_1 and μ_2 can be chosen such that $\mathrm{Im}(\mu_1) > 0$ and $\mathrm{Im}(\mu_2) > 0$. For these kinds of roots, it can be shown that

$$\ln[(z_j^+ - z_{j0})/(z_j^- - z_{j0})] = 2\pi\mathrm{i}, \tag{11}$$

where $z_{j0} = x_0 + \mu_j y_0$ $(j = 1, 2)$, $\mathrm{i} = \sqrt{-1}$ and the superscripts + and − denote the upper and lower side of the sectioning line.

The potentials for the edge dislocation at a point z_0 can be expressed as (Teutonico, 1969)

$$\Phi_1(z_1) = \frac{A}{2\pi\mathrm{i}} \ln(z_1 - z_{10}),$$
$$\Phi_2(z_2) = \frac{B}{2\pi\mathrm{i}} \ln(z_2 - z_{20}), \tag{12}$$

where A and B are complex constants. These two constants can be determined by the following conditions

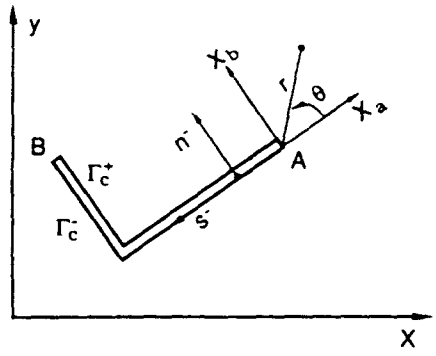

Fig. 2. Geometry and coordinate systems for a kinked crack.

$$F_x(z^+) - F_x(z^-) = 0,$$
$$F_y(z^+) - F_y(z^-) = 0, \tag{13}$$

$$u_x(z^+) - u_x(z^-) = \Delta u_1,$$
$$u_y(z^+) - u_y(z^-) = \Delta u_2, \tag{14}$$

where Δu_j is the magnitude of the dislocation. Substituting eqns (12) into eqns (7) and using eqns (13), (14), the constants A and B can be expressed as

$$A = (A_{1j} + iA_{2j})\Delta u_j,$$
$$B = (B_{1j} + iB_{2j})\Delta u_j, \tag{15}$$

where A_{kj} and B_{kj} $(k = 1, 2)$ are real constants which are given in the Appendix.

The displacements, stresses and resultant forces generated by the edge dislocation at z_0 can now be easily obtained. For example, the resultant forces at a point z can be expressed as

$$F_j(z) = F_{jk}(z, z_0)\Delta u_k + C_j, \tag{16}$$

where F_{jk} is given in the Appendix.

If a piece-wise smooth crack Γ_c (see Fig. 2) is considered and if the crack is symmetrically loaded (i.e. $\tau_j^+ = -\tau_j^-$, where τ_j is the traction on the crack surfaces), the equation for the resultant forces can in this case be written as

$$F_j(z) = \int_{\Gamma_c} F_{jk}(z, z_0) D_k(z_0)\, ds(z_0) + C_j, \tag{17}$$

where

$$D_k = \frac{\partial}{\partial s}(\Delta u_k). \tag{18}$$

The integral in eqn (17) is only performed along the lower crack line. If the point z tends to the lower side of the crack line Γ_c^-, the resultant forces can be determined from the integral of the tractions on the crack surfaces from crack tip A to the point z $(z \in \Gamma_c^-)$. Thus,

$$\int_A^z \tau_j(\lambda)\,d\lambda = \int_{\Gamma_c^-} F_{jk}(z, z_0) D_k(z_0)\,ds(z_0) + C_j. \tag{19}$$

Since only internal cracks are considered, the following constraint equation must be fulfilled

$$\int_{\Gamma_c^-} D_k(z_0)\,ds(z_0) = 0. \tag{20}$$

The problem of a piece-wise smooth crack in an anisotropic plane can now be formulated by an integral equation for the resultant forces along the crack, eqn (19), coupled to a constraint equation for the dislocation densities along the crack, eqn (20). Several features can be observed from eqn (19). First the integral kernel F_{jk} only contains a logarithmic singularity, as $z \to z_0$. Integrals with this kind of singularity are very easy to handle in the numerical calculations. Secondly, it can be proved that eqn (19) is valid for every point along the crack Γ_c. This feature will simplify the selection of collocation points along the crack line.

Apart from a few special cases, eqn (19) has to be solved numerically. In the present investigation, a boundary element technique associated with a collocation method is employed. Since the form of the integral kernels F_{jk} in eqn (19) is similar to those for cracks in an isotropic plane (Zang and Gudmundson, 1989a), the same numerical implementation is utilized in the present investigation and will only briefly be explained here.

A crack formed by two straight lines is considered. The crack is divided into two segments separated by the crack kink. Each line is then discretized into N_e elements with $N_e + 1$ nodes. Thus a double node with the same coordinate is generated at the crack kink. The line coordinate s, and the dislocation densities D_j, within an element away from the crack tip, are described by standard linear isoparametric shape functions. For instance, the interpolations for the interval $a_k a_{k+1}$ become

$$\begin{aligned} s &= M_1(\eta) s_k + M_2(\eta) s_{k+1}, \\ D_j &= M_1(\eta) D_{j,k} + M_2(\eta) D_{j,k+1}, \end{aligned} \tag{21}$$

$$\begin{aligned} M_1(\eta) &= (1-\eta)/2, \\ M_2(\eta) &= (1+\eta)/2, \end{aligned} \tag{22}$$

where s_k denotes the coordinate, $D_{j,k}$ the dislocation density at node a_k, and $|\eta| \leqslant 1$ the local coordinate for the element under consideration. For elements close to the crack tips, for example the first element $a_1 a_2$, the following interpolation is used for the dislocation densities

$$D_j = \sqrt{2/(1+\eta)}\,[M_1(\eta) D_j^* + M_2(\eta) D_{j,2}] \tag{23}$$

where $\eta = -1$ denotes the crack tip.

From the discussion above, it follows that the unknowns in eqns (19), (20) are nodal dislocation densities, which are denoted by D_j^* or $D_{j,k}$. A collocation method is then employed to solve the equations. The integrals along Γ_c^- are numerically evaluated by using Gauss–Chebyshev quadrature for non-singular parts and explicit analytical integration for singular parts. Based on the results of Sih *et al.* (1965), the asymptotic expressions for the displacement jumps, for example near crack tip A, can be expressed as

$$\begin{aligned} \Delta u_a &= 2\sqrt{2\pi r}(K_I C_{11} + K_{II} C_{12})/\pi, \\ \Delta u_b &= 2\sqrt{2\pi r}(K_I C_{21} + K_{II} C_{22})/\pi, \end{aligned} \tag{24}$$

where

$$C_{11} = \mathrm{Re}[i(-p_1\mu_2 + p_2\mu_1)\ (\mu_1 - \mu_2)],$$
$$C_{12} = \mathrm{Re}[i(-p_1 + p_2)\ (\mu_1 - \mu_2)],$$
$$C_{21} = \mathrm{Re}[i(-q_1\mu_2 + q_2\mu_1)\ (\mu_1 - \mu_2)],$$
$$C_{22} = \mathrm{Re}[i(-q_1 + q_2)\ (\mu_1 - \mu_2)]. \tag{25}$$

The stress intensity factors at crack tip A can thus be calculated afterwards as

$$K_I = \sqrt{\pi l/2}(D_a^* C_{22} - D_b^* C_{12})/C,$$
$$K_{II} = \sqrt{\pi l/2}(D_b^* C_{11} - D_a^* C_{21})/C, \tag{26}$$

where

$$C = C_{11}C_{22} - C_{12}C_{21}, \tag{27}$$

and l is the length of the first element. It should be pointed out that the material constants (β_{jk} etc.), the roots μ_1, μ_2 and the dislocation densities D_a^*, D_b^* in eqns (24), (25) should be evaluated in the coordinate system ($x_a x_b$) which is attached to the crack tip A, see Fig. 2.

3. NUMERICAL RESULTS

In this section, three numerical examples are presented to illustrate the efficiency and the reliability of the proposed method. An orthotropic material is employed for all the examples. The material is characterized by Young's moduli $E_1 = E_3 = 10$, $E_2 = 30$, Poisson's ratios $\nu_{12} = \nu_{32} = 0.25$, $\nu_{13} = 0.2$ and the shearing modulus $G_{12} = 5$. These material constants represent a typical glass fiber/epoxy composite (cf. Jones, 1975). In addition, plane strain deformation is assumed for all the tests. It is noticed that crack closure may occur in some cases under the action of applied loads. In these cases, the friction between the contact crack surfaces is neglected and the numerical algorithm presented by Zang and Gudmundson (1990) is employed to solve the contact problems.

3.1. *A straight line crack*

A straight line crack in an orthotropic plane is considered, see Fig. 3. The material principal direction E_1 is rotated an angle β with respect to the crack. A uniformly distributed normal pressure σ_0 on the crack surfaces is considered. This problem has been examined by Sih *et al.* (1965). Their results show that the stress intensity factors are independent of the material constants. Based on the potentials provided by Sih and Chen (1981), the explicit expressions for the displacement jumps along the crack can be written as

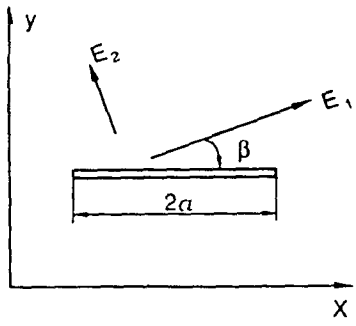

Fig. 3. A straight line crack in an orthotropic plane.

Table 1. Displacement jumps along the crack for the straight line crack in Fig. 3. The numbers within parentheses indicate the number of elements used in the calculations

s	$\Delta u_1^{(10)}$	Δu_2	$\Delta u_1^{(12)}$	Δu_2	$\Delta u_1^{(14)}$	Δu_2	Δu_1†	Δu_2†
0.000	0.0000	0.0000	0.0000	0.0000	0.0000	0.0000	0.0000	0.0000
0.027					−0.0160	0.0606	−0.0161	0.0612
0.074			−0.0260	0.0988	−0.0263	0.0998	−0.0263	0.0998
0.200	−0.0417	0.1584	−0.0421	0.1597	−0.0420	0.1595	−0.0419	0.1590
0.400	−0.0559	0.2123	−0.0559	0.2123	−0.0559	0.2124	−0.0558	0.2120
0.600	−0.0640	0.2430	−0.0640	0.2431	−0.0640	0.2431	−0.0640	0.2429
0.800	−0.0684	0.2597	−0.0684	0.2598	−0.0684	0.2599	−0.0684	0.2597
1.00	−0.0698	0.2651	−0.0698	0.2652	−0.0698	0.2652	−0.0698	0.2650
K_I	1.0022		1.0025		1.0013		1.0000	

† Results from the analytic expression.

$$\Delta u_x = 2\sigma_0(a^2-x^2)^{1/2}C_{11},$$
$$\Delta u_y = 2\sigma_0(a^2-x^2)^{1/2}C_{21}, \tag{28}$$

where $x = \pm a$ denotes the crack tips, and C_{11} and C_{21} are given in eqn (25).

Since a boundary element technique was employed in the present investigation, the present example was used to study the effect of the element sizes on the accuracy of the numerical results. The results for the displacement jumps along the crack calculated for $\beta = 45°$ and different numbers of elements are presented in Table 1 and compared to the analytical expressions of eqn (28). The results for the stress intensity factor normalized with respect to $\sigma_0\sqrt{\pi a}$ are also presented in Table 1. It is observed that the result for the stress intensity factor is insensitive to the size of the singular element. In order to achieve an accurate result for the displacement jumps near crack tips, a singular element with a size of about 3% of half crack length is recommended.

3.2. *A T-shaped crack*

A T-shaped crack in an orthotropic plane subjected to remote uniform tension σ_0 in the y direction is considered, see Fig. 4. The material principal directions are assumed to coincide with the coordinate axes. The crack is first cut into three segments at the crack kink O. The first part, from crack tip A to O, is modeled by 12 elements. The numbers of the elements for the other two branches are varied from five to 12, dependent on the lengths of the branches. In order to check the reliability of the present method, a finite element calculation using the program ADINA was carried out for the case where $b/a = 0.5$. It should be mentioned that crack closure occurs in this case in the branches parallel to the y direction.

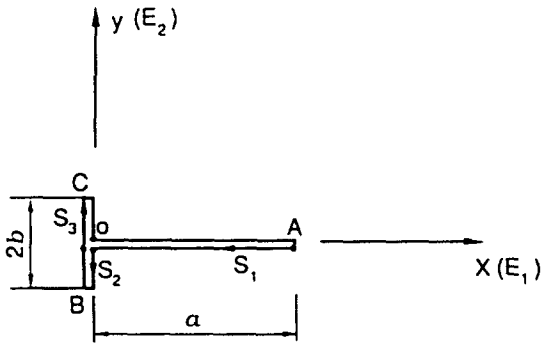

Fig. 4. A T-shaped crack in an orthotropic plane.

Table 2. Displacement jumps along the crack for the T-shaped crack

s_1	Δu_2	Δu_2†	s_2	Δu_2	Δu_2†
0	0.0000	0.0000	0	0.0509	0.0506
0.1	0.0623	0.0615	0.1	0.0448	0.0447
0.2	0.0835	0.0835	0.2	0.0386	0.0385
0.3	0.0967	0.0966	0.3	0.0315	0.0314
0.4	0.1048	0.1048	0.4	0.0222	0.0222
0.5	0.1092	0.1093	0.5	0.0000	0.0000
0.6	0.1105	0.1106			
0.7	0.1093	0.1093			
0.8	0.1062	0.1063			
0.9	0.1031	0.1029			
1.0	0.1018	0.1012			

† Results by the finite element calculation.

Table 3. Normalized stress intensity factors for the T-shaped crack

h/a	K_{IA}	K_{IB}	K_{IIB}	K_{IA}†	K_{IB}†	K_{IIB}†
0.01	0.7089	0.1260	0.1998	0.7095	0.1837	0.2401
0.05	0.7125	0.0640	0.2148	0.7145	0.0792	0.2591
0.10	0.7162	0.0247	0.2262	0.7192	0.0144	0.2767
0.20	0.7225	0.0000	0.2418	0.7284	0.0000	0.2955
0.30	0.7295	0.0000	0.2495	0.7393	0.0000	0.3026
0.40	0.7373	0.0000	0.2529	0.7512	0.0000	0.3045
0.50	0.7458	0.0000	0.2536	0.7642	0.0000	0.3022

† Results for isotropic material.

In Table 2, the results for Δu_2 along the branches AO and OB computed by the present method are compared to the finite element results. A good agreement is observed. The results for the stress intensity factors normalized with respect to $\sigma_0\sqrt{\pi a}$ computed for different ratios h/a are presented in Table 3. In order to show the effect of the material properties on the stress intensity factors, results for the same problem but with an isotropic material are also presented in Table 3. It is observed that if the length of the branches parallel to the y direction is short enough, no crack closure occurs at these two crack tips. Furthermore, it is found that the material properties have a larger effect on the results for crack tips B and C than for crack tip A.

3.3. *A crack with one kink*

A main crack with a small kinked branch subjected to remote uniform tension σ_0 in the y direction is considered, see Fig. 5. In this test, the coordinate axes are attached to the main crack, the ratio $l/a = 0.01$ is employed, the angle α between the main crack and crack kink varies from -90° to 90° and the material principal direction E_1 is rotated an angle β from the main crack. It was observed that the results for the stress intensity factors at the main crack tip were almost uninfluenced by the presence of the small branch ($K_I \approx \sigma_0\sqrt{\pi a}$, $K_{II} \approx 0$). The results for stress intensity factors at the branched tip normalized with respect

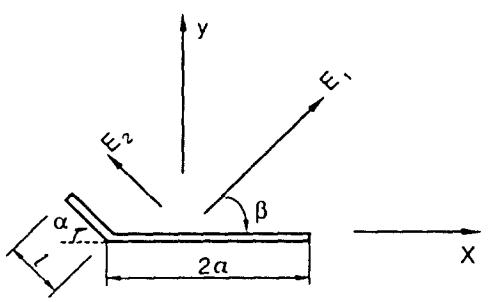

Fig. 5. A crack with one kink in an orthotropic plane.

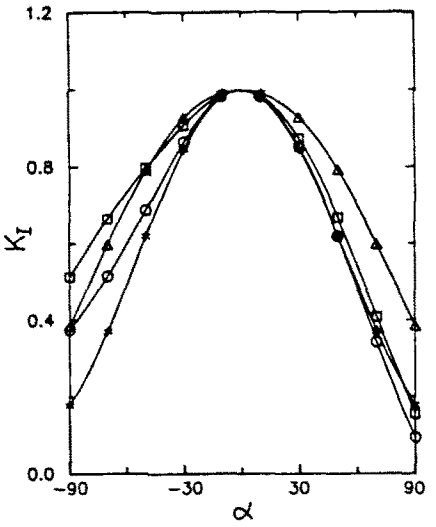

Fig. 6. Normalized stress intensity factors K_I for the kinked crack in Fig. 5. Stars denote the results calculated for $\beta = 0°$, circles for $\beta = 30°$, squares for $\beta = 60°$ and triangles for $\beta = 90°$.

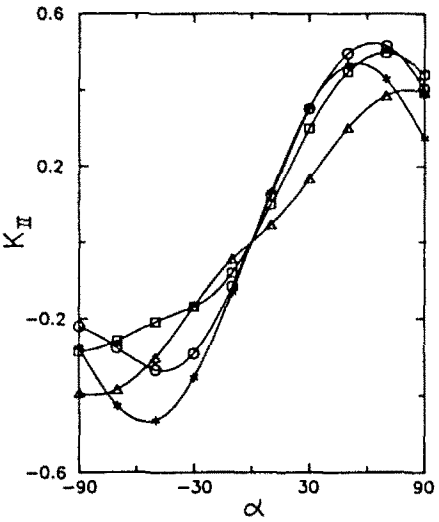

Fig. 7. Normalized stress intensity factors K_{II} for the kinked crack in Fig. 5. Stars denote the results calculated for $\beta = 0°$, circles for $\beta = 30°$, squares for $\beta = 60°$ and triangles for $\beta = 90°$.

to $\sigma_0\sqrt{\pi a}$ are presented in Fig. 6 and Fig. 7. These results can be valuable for understanding the mechanism of crack kinking in an anisotropic plane.

4. DISCUSSION

A boundary integral method for cracks in an anisotropic plane has been presented. Since the method is based on the resultant force type equation, it shows the same advantageous features which have been demonstrated for the corresponding formulations for isotropic materials. Employing the same numerical algorithm presented by Zang and Gudmundson (1990), crack closure could be taken into account without any further difficulty. The proposed method is easy to apply and valid for cracks with any geometrical configurations. The numerical tests demonstrated that the present method is an efficient and reliable tool for the solution of crack problems in an anisotropic plane.

In the present study, only infinite geometries have been considered. Cracks in a finite geometry can be handled by an application of the standard boundary element method

(BEM) for the outer boundary and the present method for crack lines, see Zang and Gudmundson (1989b) for an isotropic application.

REFERENCES

Bowie, O. L. and Freese, C. E. (1972). Central crack in plane orthotropic rectangular sheet. *Int. J. Fracture* **8**, 49–57.

Brebbia, C. A., Telles, J. C. F. and Wrobel, L. C. (1984). *Boundary Element Techniques*. Springer, Berlin.

Cheung, Y. K. and Chen, Y. Z. (1987). Solution of branch crack problems in plane elasticity by using a new integral equation approach. *Engng Fracture Mech.* **28**, 31–41.

Cinar, A. and Erdogan, F. (1982). The crack and wedging problem for an orthotropic strip. *Int. J. Fracture* **23**, 83–102.

Delale, F. and Erdogan, F. (1977). Problem of internal and edge cracks in an orthotropic strip. *J. Appl. Mech.* **44**, 237–242.

Jones, R. M. (1975). *Mechanics of Composite Materials*. McGraw-Hill, New York.

Lekhnitskii, S. G. (1981). *Theory of Elasticity of an Anisotropic Body*. English translation, Mir, Moscow.

Mishra, M. and Misra, J. C. (1983). An anisotropic strip weakened by an array of cracks. *Int. J. Engng Sci.* **21**, 187–198.

Sih, G. C. and Chen, E. P. (1981). *Cracks in Composite Materials*. Martinus Nijhoff, The Hague.

Sih, G. C., Paris, P. C. and Irwin, G. R. (1965). On cracks in rectilinearly anisotropic bodies. *Int. J. Fracture Mech.* **1**, 189–203.

Teutonico, L. J. (1969). *Dislocations in anisotropic elastic media*. In *Mathematical Theory of Dislocation* (Edited by Toshio Mura). ASME, New York.

Zang, W. L. and Gudmundson, P. (1988). A boundary integral method for internal piece-wise smooth crack problems. *Int. J. Fracture* **38**, 275–294.

Zang, W. L. and Gudmundson, P. (1989a). An integral equation method for piece-wise smooth cracks in an elastic half-plane. *Engng Fracture Mech.* **32**, 889–897.

Zang, W. L. and Gudmundson, P. (1989b). An integral equation method based on resultant forces on a piece-wise smooth crack in a finite plate. *Proc. 7th Int. Conf. on Fracture*, Houston, 2127–2134.

Zang, W. L. and Gudmundson, P. (1990). Contact problems of kinked cracks modeled by a boundary integral method. *Int. J. Numer. Methods Engng* **29**, 847–860.

APPENDIX

In a particular coordinate system, the material constants (β_{jk} etc.) and the roots of eqn (9) can be evaluated. The following values can be defined

$$\begin{aligned}
&\mu_j = \mu_{j1} + i\mu_{j2} \quad (\mu_{j2} > 0),\\
&p_j = p_{j1} + ip_{j2} = \beta_{11}\mu_j^2 + \beta_{12} - \beta_{16}\mu_j \quad (j = 1, 2),\\
&q_j = q_{j1} + iq_{j2} = \beta_{12}\mu_j + \beta_{22}/\mu_j - \beta_{26},
\end{aligned} \tag{A1}$$

where μ_{j1}, p_{j1}, q_{j1} and μ_{j2}, p_{j2}, q_{j2} denote real and imaginary parts respectively.

The constants A ($A = A_{1k} + iA_{2k}$) and B ($B = B_{1k} + iB_{2k}$) in eqn (15) can be expressed as

$$\begin{aligned}
A_{11} &= +\mu_{22}E_{22}/(2E),\\
A_{12} &= -\mu_{22}E_{12}/(2E),\\
A_{21} &= -\mu_{22}E_{21}/(2E),\\
A_{22} &= +\mu_{22}E_{11}/(2E),\\
B_{11} &= -A_{11},\\
B_{12} &= -A_{12},\\
B_{21} &= -\mu_{12}A_{21}/\mu_{22} + (\mu_{11} - \mu_{21})A_{11}/\mu_{22},\\
B_{22} &= -\mu_{12}A_{22}/\mu_{22} + (\mu_{11} - \mu_{21})A_{12}/\mu_{22},
\end{aligned} \tag{A2}$$

where

$$\begin{aligned}
E_{11} &= \mu_{22}(p_{11} - p_{21}) - p_{22}(\mu_{11} - \mu_{21}),\\
E_{12} &= -\mu_{22}p_{12} + \mu_{12}p_{22},\\
E_{21} &= \mu_{22}(q_{11} - q_{21}) - q_{22}(\mu_{11} - \mu_{21}),\\
E_{22} &= -\mu_{22}q_{12} + \mu_{12}q_{22},\\
E &= E_{11}E_{22} - E_{12}E_{21}.
\end{aligned} \tag{A3}$$

The integral kernels F_{jk} in eqn (19) can be given as

$$F_{1k} = +\frac{1}{\pi}[(\mu_{11}A_{2k}+\mu_{12}A_{1k})\ln(R_1)+(\mu_{11}A_{1k}-\mu_{12}A_{2k})\theta_1+(\mu_{11}B_{2k}+\mu_{12}B_{1k})\ln(R_2)+(\mu_{11}B_{1k}-\mu_{12}B_{2k})\theta_2],$$

$$F_{2k} = \frac{-1}{\pi}[A_{2k}\ln(R_1)+A_{1k}\theta_1+B_{2k}\ln(R_2)+B_{1k}\theta_2]. \tag{A4}$$

where

$$\begin{aligned} R_{j1} &= (x-x_0)+\mu_{j1}(y-y_0),\\ R_{j2} &= \mu_{j2}(y-y_0),\\ R_j^2 &= (R_{j1}^2+R_{j2}^2),\\ \theta_j &= \cos^{-1}(R_{j1}/R_j) \quad (j=1,2). \end{aligned} \tag{A5}$$